

Supplementary Materials for

Hepatocyte Notch activation induces liver fibrosis in nonalcoholic steatohepatitis

Changyu Zhu, KyeongJin Kim, Xiaobo Wang, Alberto Bartolome, Marcela Salomao, Paola Dongiovanni, Marica Meroni, Mark J. Graham, Katherine P. Yates, Anna Mae Diehl, Robert F. Schwabe, Ira Tabas, Luca Valenti, Joel E. Lavine, Utpal B. Pajvani*

*Corresponding author. Email: up2104@columbia.edu

Published 21 November 2018, *Sci. Transl. Med.* **10**, eaat0344 (2018)

DOI: 10.1126/scitranslmed.aat0344

This PDF file includes:

Materials and Methods

- Fig. S1. HES1 in α SMA⁺ myofibroblasts and CK7⁺ cholangiocytes in human livers.
 - Fig. S2. NASH diet feeding induces steatohepatitis and fibrosis in WT mice.
 - Fig. S3. Characterization of NASH diet-fed *L-DNMAM* mice.
 - Fig. S4. Characterization of NASH diet-fed *L-Ncst* mice.
 - Fig. S5. Characterization of *L-DNMAM* mice on NASH diet for 32 weeks.
 - Fig. S6. Hepatocyte Notch loss of function does not protect from MCD-induced liver fibrosis.
 - Fig. S7. Characterization of NASH diet-fed Notch gain-of-function mice.
 - Fig. S8. Characterization of chow-fed *L-NICD* male mice.
 - Fig. S9. Characterization of chow-fed *L-NICD* female mice.
 - Fig. S10. Loss of hepatocyte Notch activity does not affect DRs.
 - Fig. S11. Hepatocyte Notch activity regulates *Spp1* and *Sox9* expression.
 - Fig. S12. Additional characterization of AAV8-H1-sh*Spp1*-transduced mice.
 - Fig. S13. Characterization of GSI-treated, NASH diet-fed mice.
 - Fig. S14. Additional characterization of GSI- and ASO-treated mice.
 - Fig. S15. Comparison of saline- and control ASO-treated mice.
 - Fig. S16. Model of hepatocyte Notch action to increase NASH-associated fibrosis.
 - Table S1. Demographic and clinical features of PIVENS patients.
 - Table S2. Demographic and clinical features of patients with suspected NASH.
 - Table S3. Sequences of quantitative polymerase chain reaction primers used in the experiments.
- References (69–76)

Materials and Methods

γ -secretase inhibitor (GSI) and Antisense oligonucleotide (ASO) studies. GSI was used as previously described (15, 54, 69). In short, DBZ (Syncom) was suspended in vehicle [0.5% Methocel E4M (wt/vol, Colorcon) and 0.1% (vol/vol) Tween-80 (Sigma)]. Immediately prior to injection, DBZ was sonicated for 2 minutes to suspension, and administered once daily by intraperitoneal injection to male C57BL/6J mice for 7 days at 10 μ mol/kg body weight, or every other day for 20 days at 5 μ mol/kg body weight. Control ASO (GGCCAATACGCCGTCA) and *Nicastrin* ASO (CAGAATAGACTTCCTC) were synthesized by Ionis Pharmaceuticals (26). Single strand ASOs do not require expients, with uptake facilitated by both passive diffusion and receptor-mediated endocytic mechanisms (70). Both ASOs were dissolved in saline and administered by intraperitoneal injection to male C57BL/6J mice at a dose of 25 mg/kg of body weight once weekly for 8 weeks prior to sacrifice.

AAV and adenovirus experiments. Adeno-associated virus subtype 8 (AAV8) containing hepatocyte-specific *Cre* recombinase (AAV-TBG-*Cre*, AV-8-PV1091) and control vector (AAV-TBG-*LacZ*, AV-8-PV0142) were obtained from the Penn Vector Core and administered to 8-week-old *Rosa*^{DNMAM} and *Rosa*^{NICD} mice by tail vein injection at a dose of 1.5×10^{11} genome copies/mouse, 1 week prior to initiation of NASH diet, unless otherwise noted. AAV8-shRNA targeting mouse *Spp1* was made by annealing complementary oligonucleotides (5'-CACCACTCTTAGCTTAGTCTGTTGTTTCAAGA GAACAACAGACTAAGCTAAGAG-3'), which were ligated into the self-complementary AAV8-RSV-GFP-H1 vector (71). The final construct AAV8-H1-sh*Spp1* was amplified by the Salk Institute Gene Transfer, Targeting, and Therapeutics Core. Ad-NICD and Ad-GFP adenoviruses have been described (69). We transduced primary hepatocytes at a multiplicity of infection (MOI) of 10 to achieve 90% to 100% infection efficiency as assessed by GFP-positive hepatocytes.

Cell isolation. Hepatocytes were isolated as previously described (72). In brief, mice were anaesthetized with ketamine/xylazine (Sigma) and inferior vena cava cannulated with a 22-gauge catheter (Terumo Medical). After transection of the portal vein, EGTA-containing perfusion buffer was

infused followed by a type I collagenase solution (Worthington Biochemical). After collagenase digestion, the liver was removed, minced and further digested in pronase solution to release NPCs. Individual cells were filtered through a 100 μ m cell strainer then 50 g centrifugation to separate pelleted hepatocytes, which was further purified by Percoll gradient, and NPC-containing supernatant that was subsequently pelleted by 580 g centrifugation and subjected to 14.5% Nycodenz gradient for further purification. In some experiments, including isolation of hepatocytes from NASH diet-fed WT, *L-DNMAM*, *L-NICD* and Notch-Venus reporter mice, hepatocytes were purified by cell size (FSC) and granularity (SSC) as described (73). Total NPCs were further fractionated by FACS to HSCs (via Vitamin A fluorescence (74)) and liver myeloid cells [with CD45-APC (BD Biosciences, #559864) and CD11b-FITC (BD Biosciences, #553310)].

Quantitative reverse-transcription PCR. RNA was extracted from liver with Trizol (ThermoFisher) or isolated cells with NucleoSpin RNA (Clontech), prior to cDNA synthesis (ThermoFisher) and quantitative PCR with a DNA Engine Opticon 2 System (Bio-Rad) and Power SYBR Green (ThermoFisher). mRNA expression was normalized to housekeeping genes using the $\Delta\Delta C(t)$ method and presented as relative transcript expression (arbitrary unit). For mouse mRNAs, the expression was normalized to *Tbp*. Absolute mRNA copy numbers were determined for each Notch receptor using primer-specific standard curves, then normalized to *36b4*, and presented as relative transcript levels (copy number/ 10^3 *36b4*). For human mRNAs, the expression was normalized to either *18S* (PIVENS) or *ACTB* (cross-sectional analysis). Primer sequences are listed in table S3.

Serum transaminase measurement. Serum ALT (Teco Diagnostics) and AST (ThermoFisher, TR70121) were measured and analyzed according to the manufacturer's instructions.

Hepatic lipid measurement. Liver lipids were extracted by the Folch method (75), and hepatic triglyceride (Thermo) and Cholesterol E (Wako) measured using colorimetric assays based on the manufacturers' protocols.

Immunohistochemistry and quantification. Following sacrifice and rapid excision of the liver, tissues were fixed in 4% paraformaldehyde at 4 °C for 24 hours and later embedded in paraffin, sectioned into 5 µm thickness slides which were deparaffinized, rehydrated and stained for immunohistochemical analysis, including H&E, PAS and Sirius red staining. A minimum of 15 low-power fields of Sirius red images per mouse were taken using a polarized light filter and analyzed by Adobe Photoshop as previously described (76). PAS staining quantification was done by taking 5-8 non-overlapping images in randomly chosen fields per mouse intestinal section from at least 5 animals per experiment, then directly counting staining-positive cells. Images for quantification and representative images were taken with a Zeiss light microscope coupled with an AxioCam camera (MR3; Carl Zeiss).

Immunofluorescence and quantification. For immunostaining of human liver biopsies, paraffinized slides were deparaffinized and rehydrated as previously described (16), prior to antigen retrieval by incubating slides in HistoVT One (Nacalai) in a 100 °C steam cooker for 20 minutes. Slides were then incubated at 4 °C overnight with primary antibodies against HES1 (Santa Cruz, sc-25392, 1:100), HNF4α (Santa Cruz, sc-6556, 1:100), aSMA (DAKO, M085101-2, 1:300) and CK7 (DAKO, M701801-2, 1:300), then secondary antibodies (anti-mouse Alexa Fluor 488, Invitrogen, A-21202, 1:500; anti-rabbit Alexa Fluor 555, Invitrogen, A-31572, 1:500; donkey anti-goat Alexa Fluor 647, Invitrogen, A-21447, 1:500) prior to mounting with SlowFade Diamond Antifade DAPI Mountant (ThermoFisher, S36973).

For immunostaining of mouse livers, after harvest, tissues were fixed in 4% paraformaldehyde, followed by incubation in 30% sucrose overnight for cryopreservation. Tissues were embedded with OCT (Tissue Tek), stored at -80 °C, then slides prepared with 7 µm thickness sectioned. Antigen retrieval was performed by incubating frozen slides in HistoVT One solution (Nacalai) in a 70 °C water bath for 20 minutes. Slides were incubated at 4 °C overnight with primary antibodies

against Hes1 (Santa Cruz, sc-25392, 1:100), HNF4 α (Santa Cruz, sc-6556, 1:100), CD45 (BD Biosciences, 550539, 1:100), GFP (Abcam, ab6673, 1:200), CK19 (Abcam, ab52625, 1:300), Opn (R&D Systems, AF808, 1:200) and Alexa Fluor 488-, 555- and 647-conjugated secondary antibodies (Invitrogen). TUNEL staining was performed by using the in situ cell death detection kit (Sigma, #12156792910) based on the manufacturer's protocol.

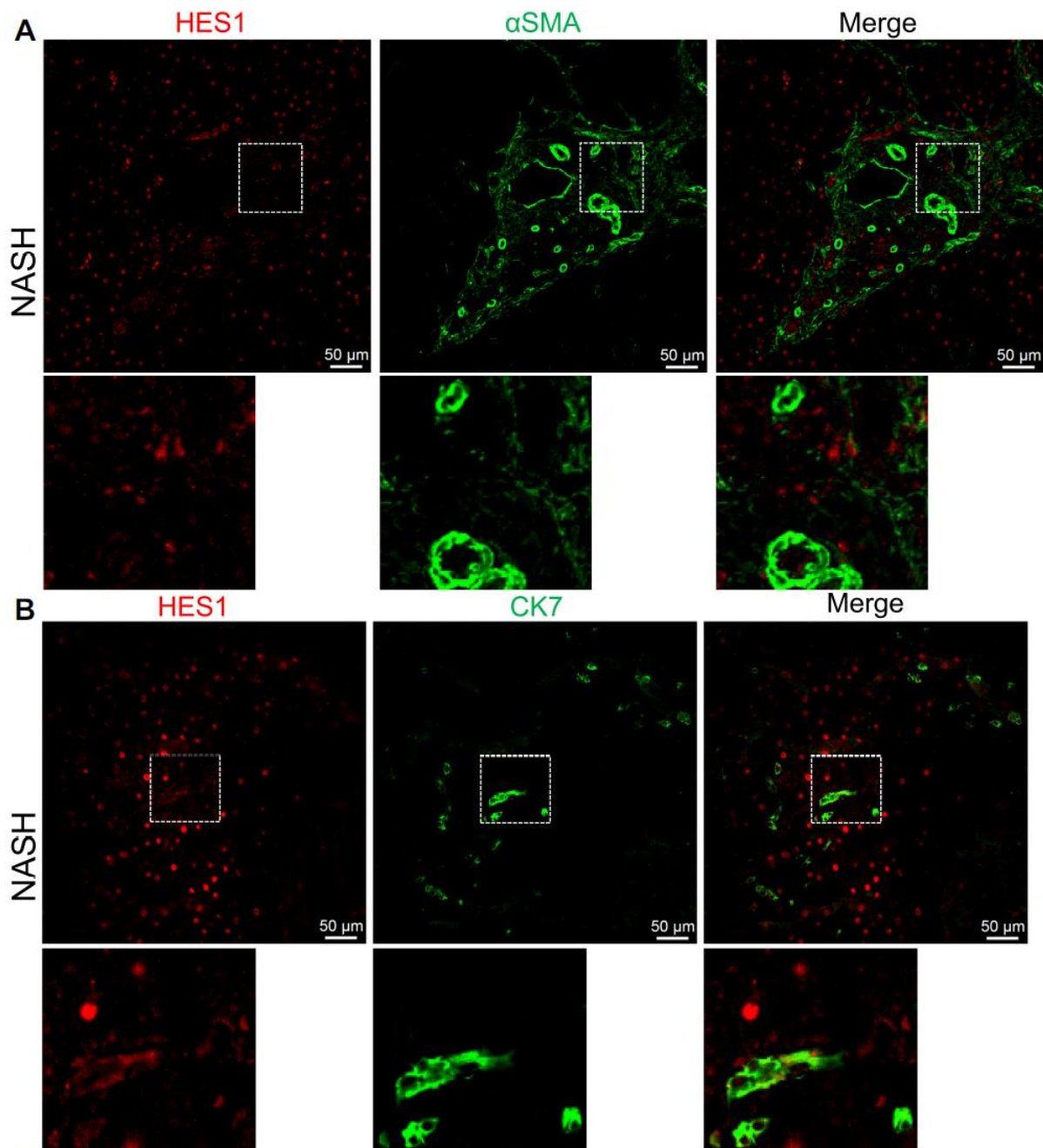
For quantification, images of 15 to 20 non-overlapping and randomly chosen fields per section were taken from at least 5 animals per experiment with a Zeiss Confocal microscope (Axio Observer Z1 with LSM 710 scanning module). Quantification was performed by directly counting staining-positive cells on ZEN 2 software; for nuclear antigens (HES1 and HNF4 α), only cells with a clear nuclear staining pattern were counted.

Western Blotting. Liver tissues were lysed in a Triton-based lysis buffer and whole-cell lysates obtained by subsequent centrifugation. Lysate, or hepatocyte conditioned media (CM) was mixed with SDS sample buffer prior to SDS-PAGE. Immunoblots were conducted as previously described (72) with primary antibodies against Notch1 (Cell signaling, 4380, 1:1000), Notch2 (Cell signaling, 5732, 1:1000), α -Tubulin (Sigma, T5168, 1:3000), β -Actin (Cell signaling, 4970, 1:2000) and Opn (R&D Systems, AF808, 1:2000).

siRNA and neutralizing antibody in vitro experiments. siRNA against mouse *Spp1* (GAAGAUGAUAGGUAUCUGAAAUUCC), *Sox9* (CUACUCCACCUUCACUUACAUGAAC), *Hes1* (CUCUUCUGACGGACACUAAAAACGA) and scrambled control (CGUUAUCGCGUAUAAUACGCGUAT) were purchased from Integrated DNA Technologies, and transfected into primary hepatocytes derived from 8-week-old C57BL/6J mice using Lipofectamine 300 (ThermoFisher, #L3000015) according to the manufacturer's instructions, with simultaneous Ad-GFP or Ad-NICD adenoviral transduction. In some experiments, transfected hepatocytes were cultured in serum-free DMEM for 24 hours for CM collection. In parallel, HSCs from other 8-week-old C57BL/6J

mice were isolated as described (74) and serum-starved overnight before CM incubation. Alternatively, Opn neutralizing antibody (R&D Systems, AF808) was added directly into the CM at the recommended ND_{50} of 1 $\mu\text{g}/\text{mL}$ prior to HSC incubation.

Cytokine array. 100 μl CM from Ad-GFP or Ad-NICD-transduced (n=3 wells/sample) primary hepatocytes isolated from WT mice were pooled, then applied to a Proteome Profiler Mouse XL Cytokine Array kit (R&D Systems, ARY028) to survey 111 different secreted cytokines. Each cytokine has technical duplicates as well as two biological replicates. Array signals were analyzed using ImageJ (NIH), and the average pixel density used to compare differences between groups.



C Average percentage of HES1+ cells

Cell type	Normal	SS	NASH
Hepatocytes (HNF4 α +)	4%	10%	52%
Myofibroblasts (α SMA+)	35%	35%	30%
Cholangiocytes (CK7+)	65%	70%	80%

Fig. S1. HES1 in α SMA⁺ myofibroblasts and CK7⁺ cholangiocytes in human livers. (A)

Representative images of HES1 (red) colocalization with α SMA (green)-positive myofibroblasts or (B)

CK7 (green)-positive cholangiocytes in liver biopsies from patients with NASH. (C) Quantitation of %HES1⁺ cells in histologically normal livers, livers with simple steatosis (SS) or NASH ($n = 3$ per group).

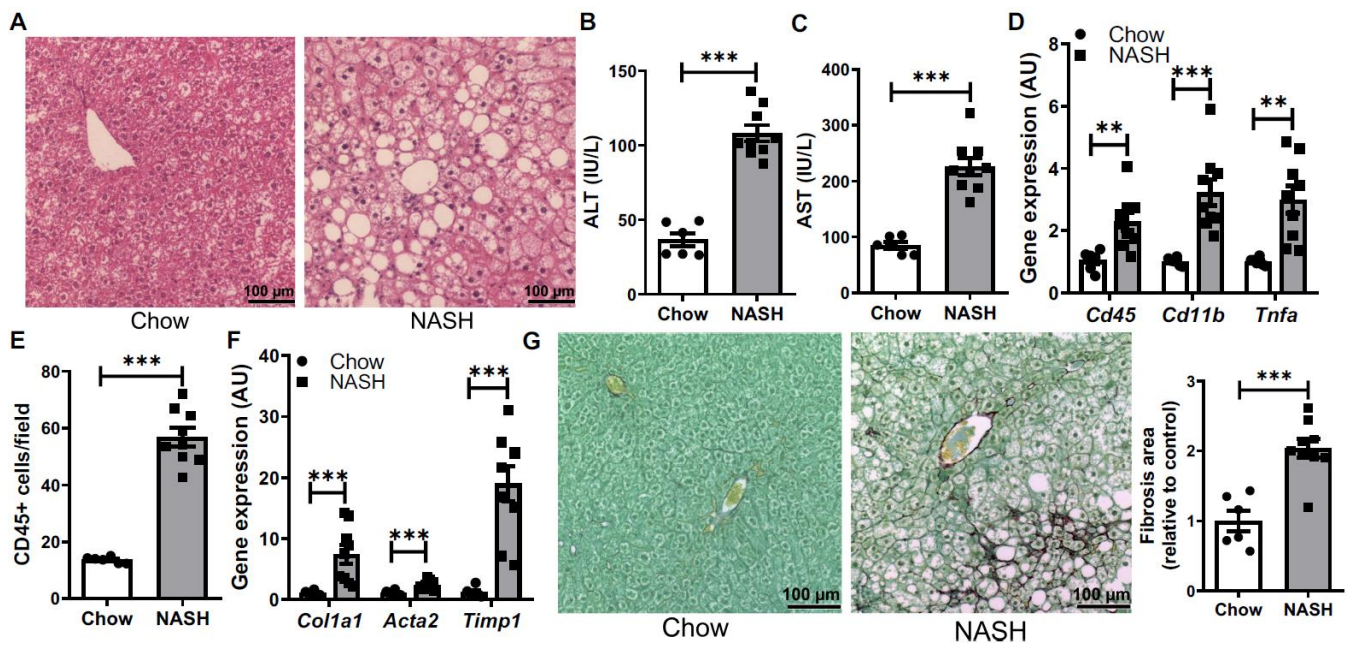


Fig. S2. NASH diet feeding induces steatohepatitis and fibrosis in WT mice. (A) Liver H+E staining, (B) serum ALT and (C) AST, (D) liver inflammatory gene expression, (E) CD45⁺ cell infiltration, (F) fibrogenic gene expression and (G) collagen deposition in WT mice fed normal chow or NASH diet for 16 weeks ($n = 6$ per group). ** $P < 0.01$ and *** $P < 0.001$ as compared to chow-fed control WT mice by 2-tailed t tests (2 groups). AU, arbitrary unit. All data are shown as the means \pm SEM.

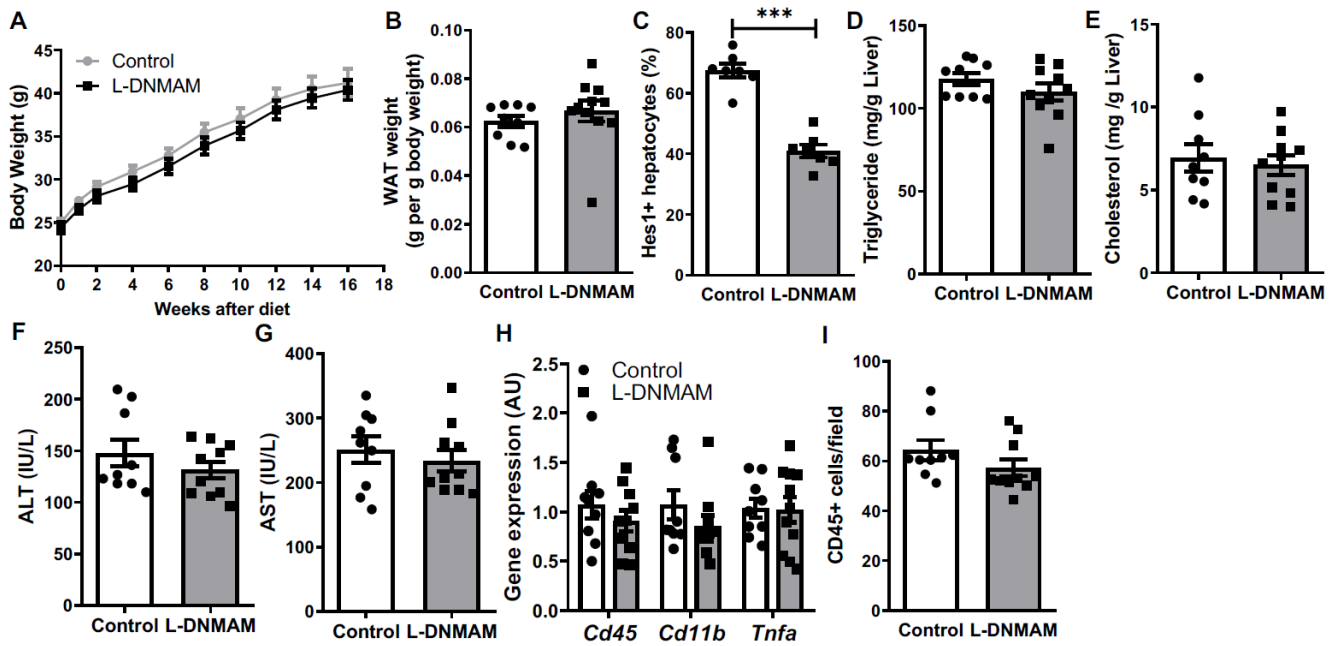


Fig. S3. Characterization of NASH diet-fed *L-DNMAM* mice. (A) Body weight curve, (B) epididymal white adipose tissue (WAT) weight, (C) staining quantification of Hes1⁺ hepatocytes (related to Fig. 2C), (D) liver triglyceride and (E) cholesterol, (F) serum ALT and (G) AST, (H) liver inflammatory gene expression and (I) hepatic CD45⁺ cell infiltrate in Cre⁻ controls and *L-DNMAM* mice fed NASH diet for 16 weeks ($n = 9$ to 10 per group). *** $P < 0.001$ as compared to Cre⁻ controls by 2-tailed t tests (2 groups). AU, arbitrary unit. All data are shown as the means \pm SEM.

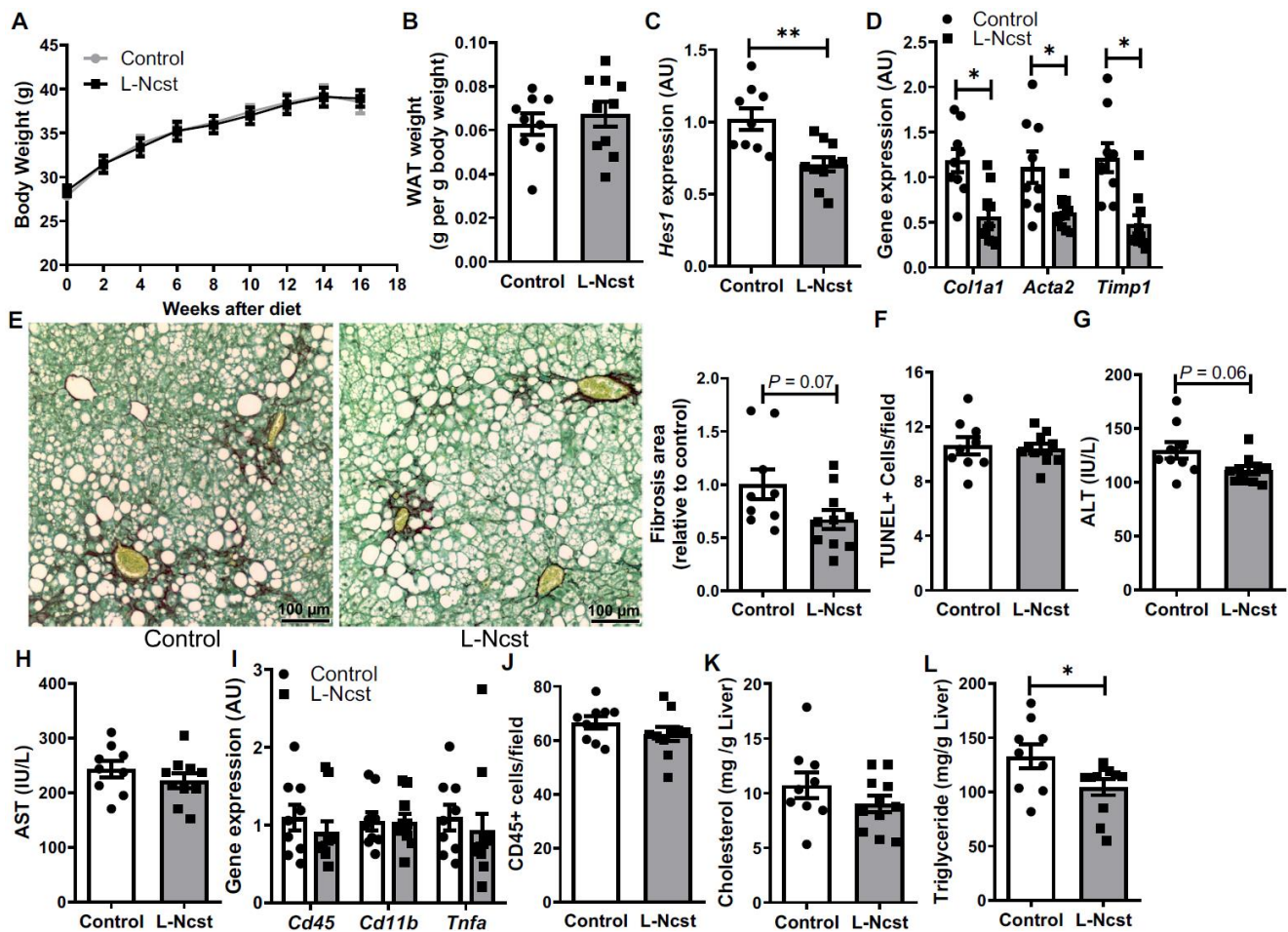


Fig. S4. Characterization of NASH diet-fed *L-Ncst* mice. (A) Body weight curve, (B) epididymal WAT weight, (C) liver *Hes1* and (D) fibrogenic gene expression, (E) liver collagen deposition, (F) staining quantification of liver TUNEL+ cells, (G) serum ALT and (H) AST, (I) liver inflammatory gene expression, (J) CD45⁺ cell infiltrate, (K) cholesterol and (L) triglyceride in Cre⁻ and *L-Ncst* mice fed NASH diet for 16 weeks ($n = 9$ to 10 per group). * $P < 0.05$ as compared to Cre⁻ controls by 2-tailed t tests (2 groups). AU, arbitrary unit. All data are shown as the means \pm SEM.

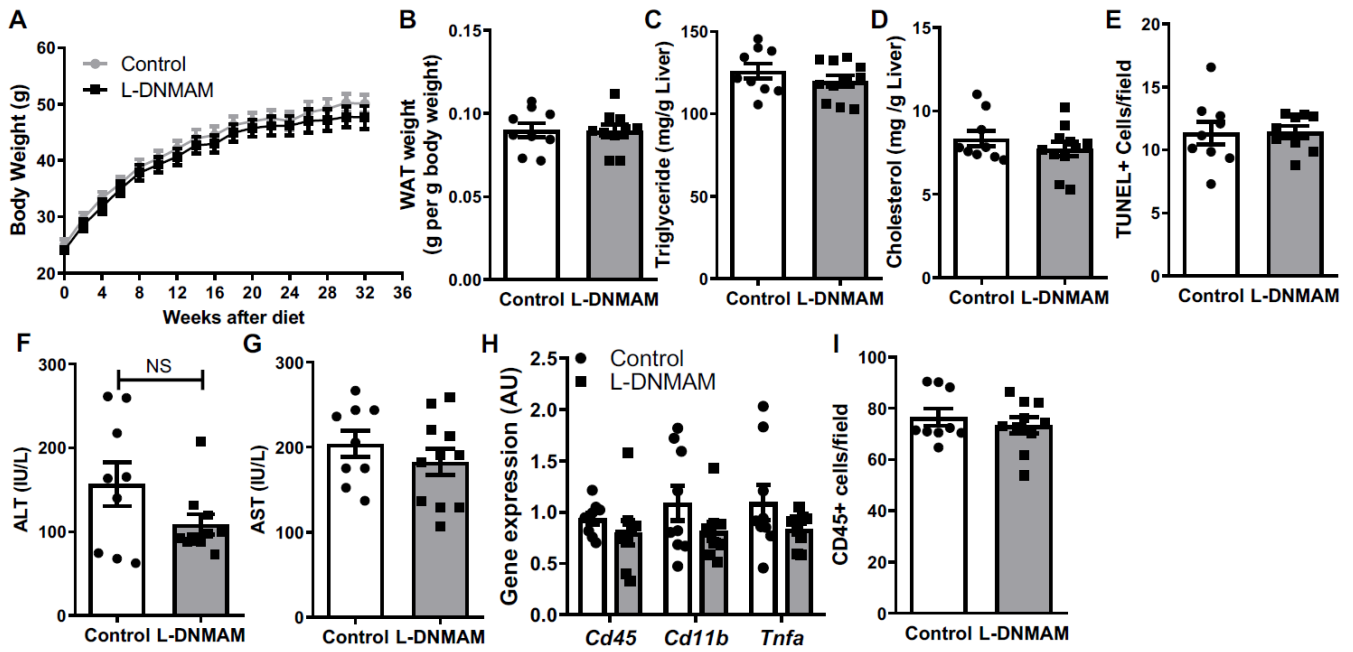


Fig. S5. Characterization of *L-DNMAM* mice on NASH diet for 32 weeks. (A) Body weight curve, (B) epididymal WAT weight, (C) liver triglyceride and (D) cholesterol, (E) quantification of liver TUNEL+ cells, (F) serum ALT and (G) AST, (H) liver inflammatory gene expression and (I) CD45⁺ cell infiltrate in Cre⁻ controls and *L-DNMAM* mice with Cre⁻ mediated recombination induced 16 weeks after NASH diet initiation ($n = 9$ per group). 2-tailed t tests were performed to compare the two groups. NS, not significant. AU, arbitrary unit. All data are shown as the means \pm SEM.

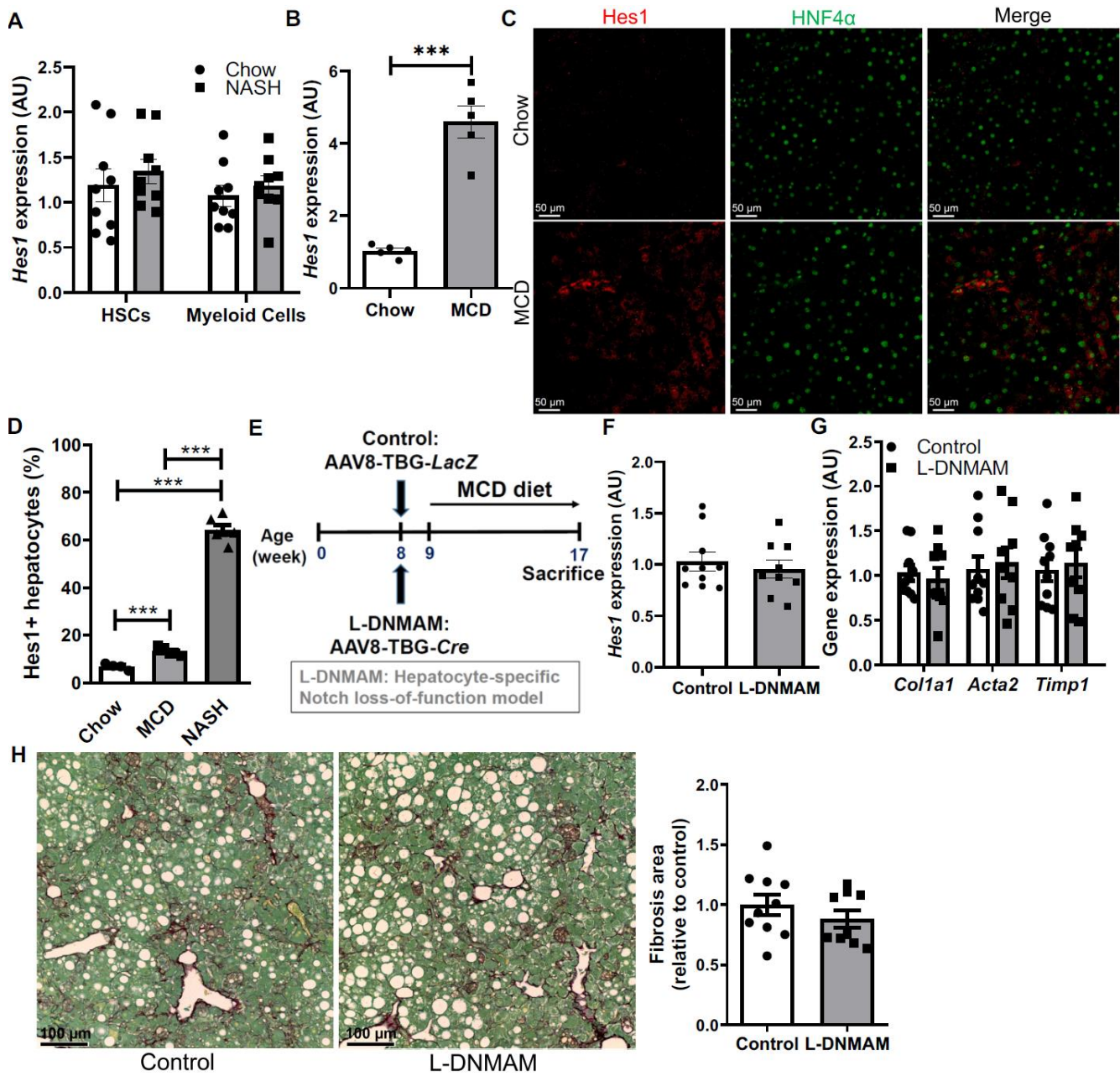


Fig. S6. Hepatocyte Notch loss of function does not protect from MCD-induced liver fibrosis.

(A) *Hes1* expression in FACS-sorted HSCs (hepatic stellate cells) and myeloid cells from chow and NASH diet-fed WT mice ($n = 9$ per group). (B) Liver *Hes1* expression and (C) representative images of *Hes1* and HNF4 α immunofluorescence in chow and MCD diet-fed mice, with (D) quantification of nuclear *Hes1*⁺ hepatocytes relative to NASH diet-fed mice ($n = 5$ per group). (E) 8-week old *Rosa*^{DNMAM} male mice were transduced with AAV8-TBG-*LacZ* (Control) or AAV8-TBG-*Cre* (*L-DNMAM*) prior to 8 weeks of MCD diet-feeding ($n = 9$ to 10 per group). (F) Liver *Hes1*, (G) fibrogenic gene expression and

(H) collagen deposition in MCD-fed Cre⁻ and *L-DNMAM* mice. ** $P < 0.01$ and *** $P < 0.001$ as compared to the indicated controls by 2-tailed t tests (2 groups) or one-way ANOVA followed by post-hoc t tests (3 groups). AU, arbitrary unit. All data are shown as the means \pm SEM.

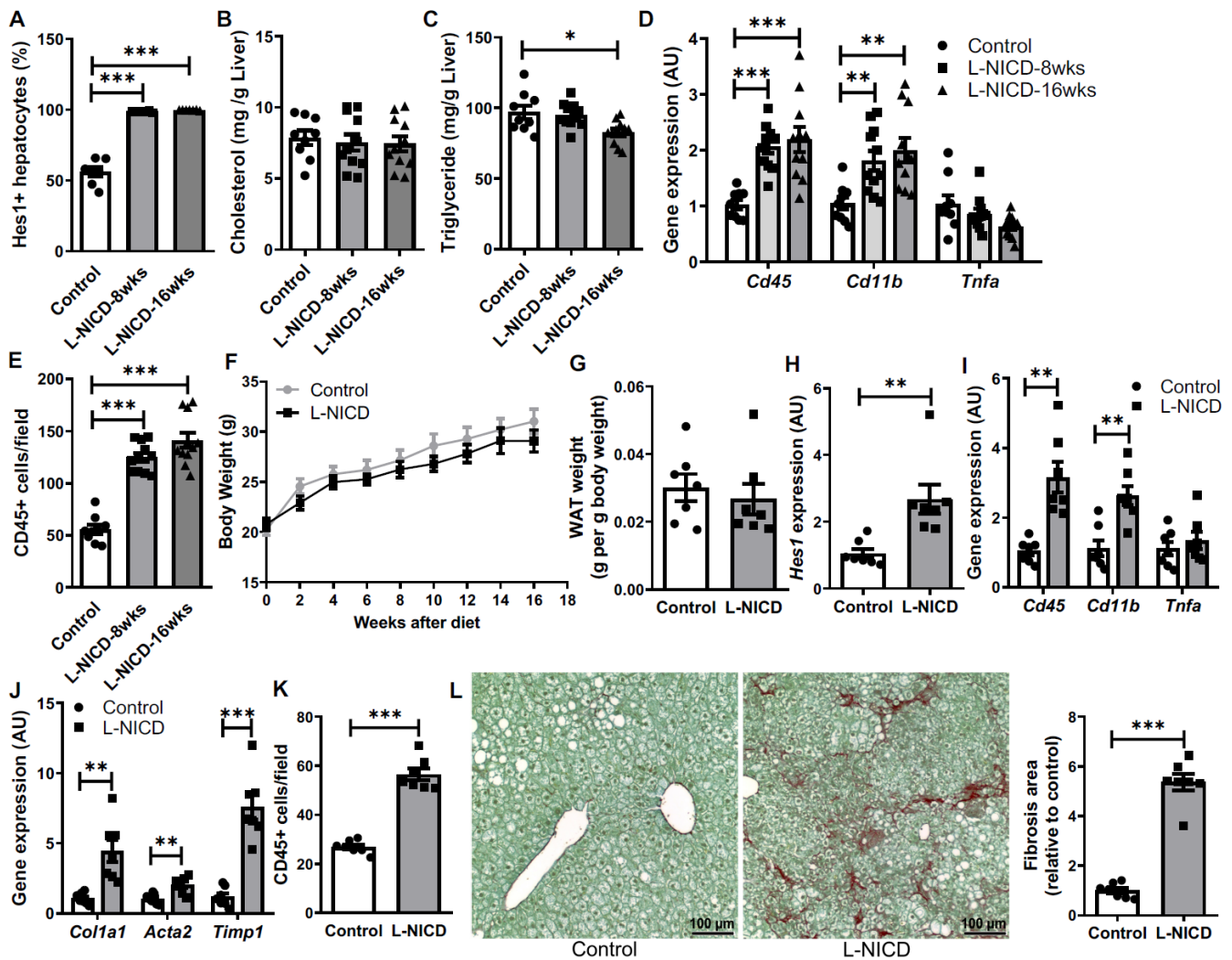


Fig. S7. Characterization of NASH diet-fed Notch gain-of-function mice. (A) Quantification of Hes1⁺ hepatocytes (related to Fig. 3C), (B) liver cholesterol, (C) triglyceride, (D) inflammatory gene expression and (E) CD45⁺ cell infiltrate in Cre⁻ and *L-NICD* male mice fed NASH diet for 16 weeks ($n = 9$ to 11 per group). (F) Body weight curve, (G) perigonadal WAT weight, (H) liver *Hes1*, (I) inflammatory and (J) fibrogenic gene expression, (K) CD45⁺ infiltrate and (L) collagen deposition in Cre⁻ and *L-NICD* female mice fed NASH diet for 16 weeks ($n = 7$ per group). * $P < 0.05$, ** $P < 0.01$ and *** $P < 0.001$ as compared to Cre⁻ controls by 2-tailed t tests (2 groups) or one-way ANOVA followed by post-hoc t tests (3 groups). AU, arbitrary unit. All data are shown as the means \pm SEM.

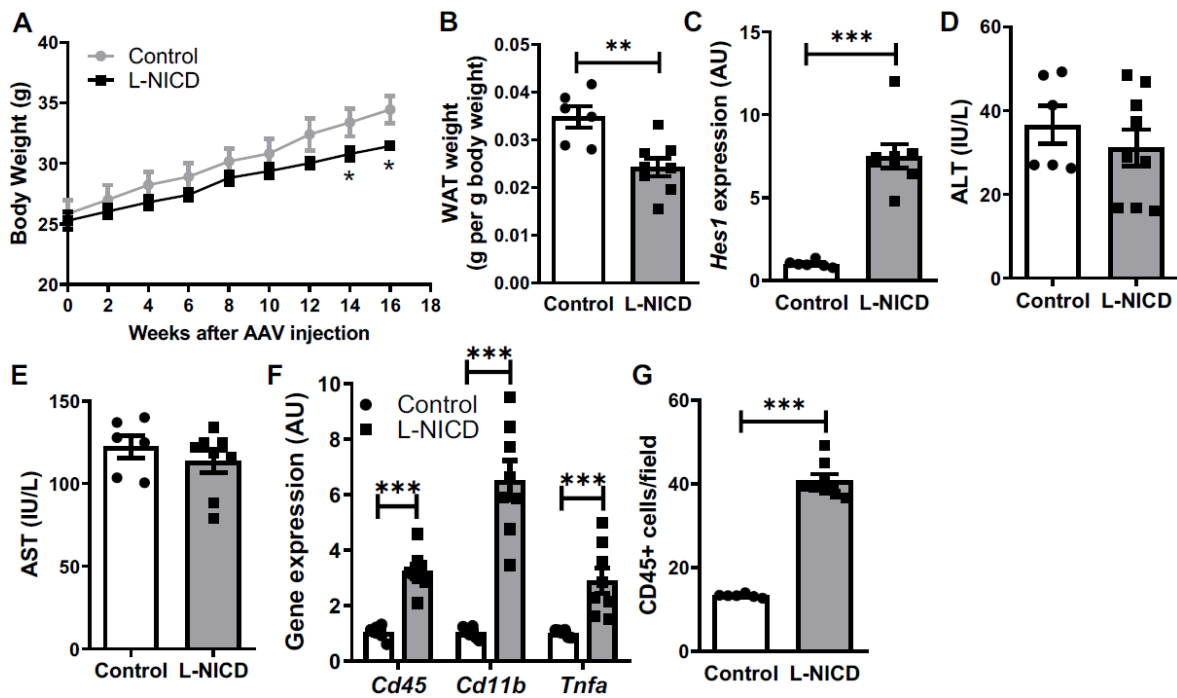


Fig. S8. Characterization of chow-fed *L-NICD* male mice. (A) Body weight curve, (B) epididymal WAT weight, (C) liver *Hes1*, (D) serum ALT and (E) AST, (F) liver inflammatory gene expression and (G) CD45⁺ cell infiltrate in chow-fed Cre⁻ and *L-NICD* male mice ($n = 6$ to 8 per group). ** $P < 0.01$ and *** $P < 0.001$ as compared to Cre⁻ controls by 2-tailed t tests (2 groups). AU, arbitrary unit. All data are shown as the means \pm SEM.

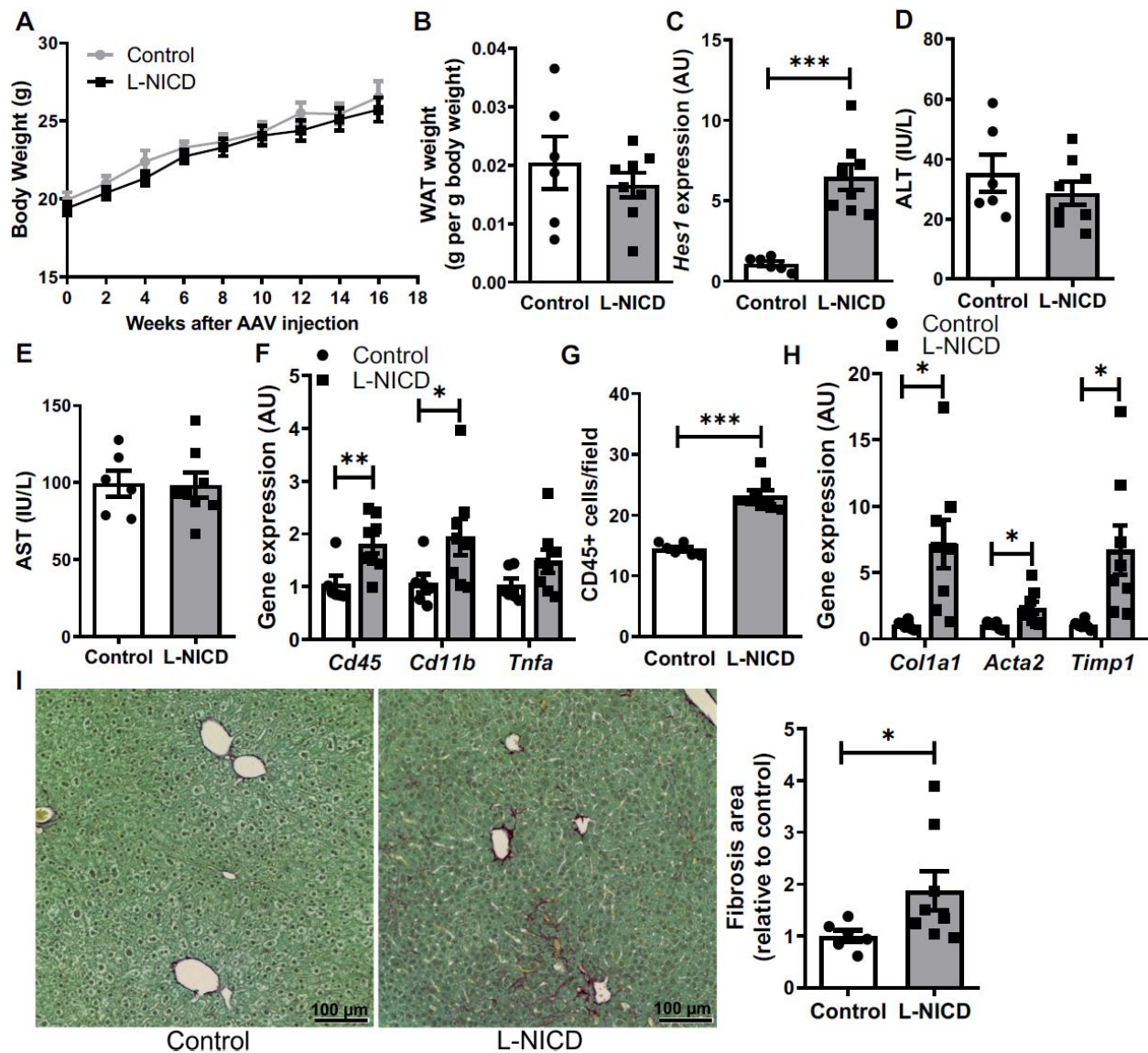


Fig. S9. Characterization of chow-fed *L-NICD* female mice. (A) Body weight curve, (B) perigonadal WAT weight, (C) liver *Hes1*, (D) serum ALT and (E) AST, (F) liver inflammatory gene expression, (G) CD45⁺ cell infiltrate, (H) fibrogenic gene expression and (I) collagen deposition in chow-fed Cre⁻ and *L-NICD* female mice ($n = 7$ per group). * $P < 0.05$, ** $P < 0.01$ and *** $P < 0.001$ as compared to Cre⁻ controls by 2-tailed t tests (2 groups). AU, arbitrary unit. All data are shown as the means \pm SEM.

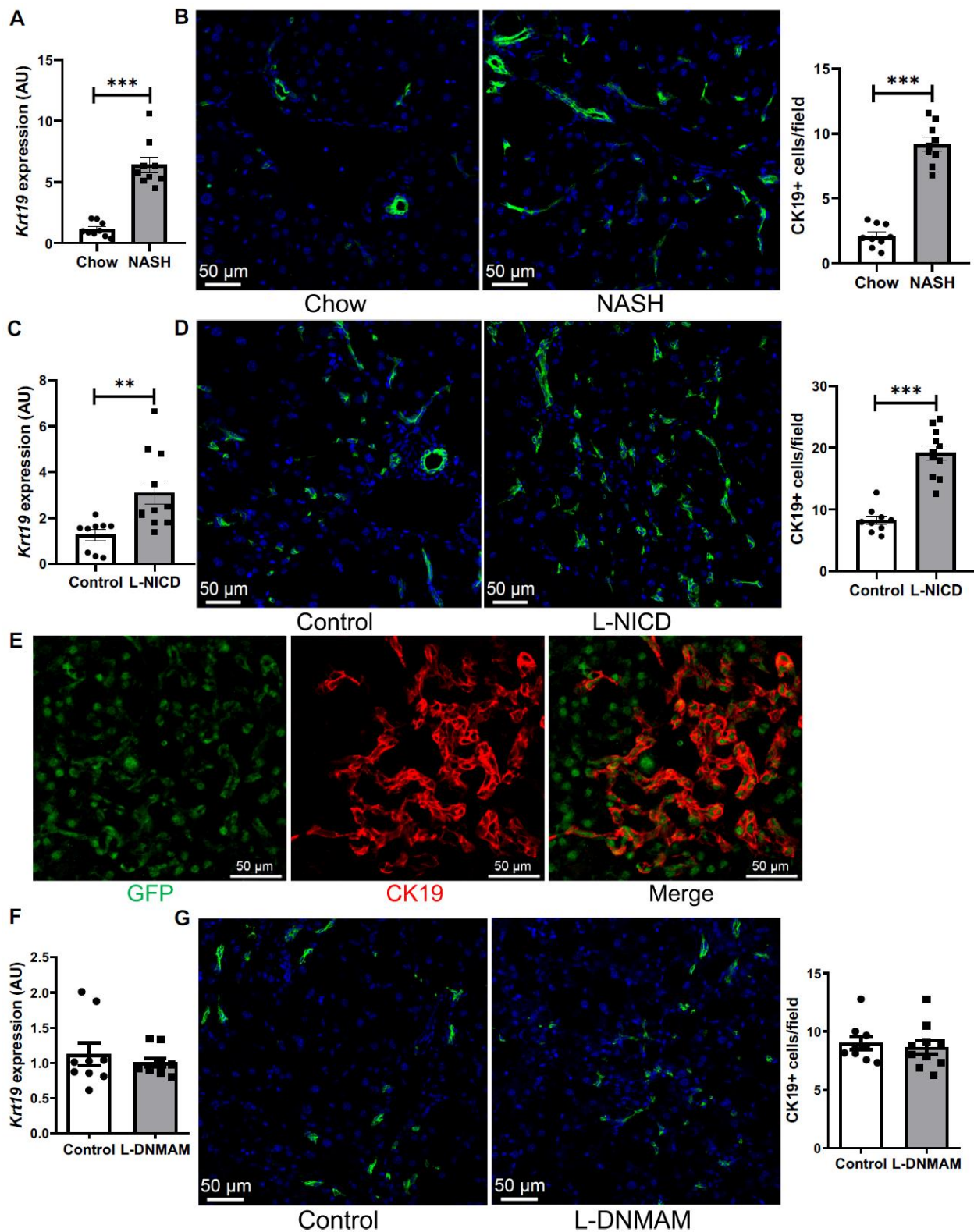


Fig. S10. Loss of hepatocyte Notch activity does not affect DRs. (A) Liver *Krt19* expression and (B) CK19⁺ cells in WT mice fed NASH diet for 16 weeks ($n = 9$ per group). (C) Liver *Krt19* expression and (D) CK19⁺ cells in Cre⁻ and L-NICD mice fed NASH diet for 16 weeks ($n = 9$ to 11 per group). (E)

Representative images of hepatocyte-derived GFP⁺/CK19⁺ cholangiocytes in *L-NICD* mice. **(F)** Liver *Krt19* expression and **(G)** CK19⁺ cells in *L-DNMAM* mice fed NASH diet for 16 weeks ($n = 9$ to 10 per group). * $P < 0.05$ and *** $P < 0.001$ as compared to the indicated controls by 2-tailed t tests (2 groups). AU, arbitrary unit. All data are shown as the means \pm SEM.

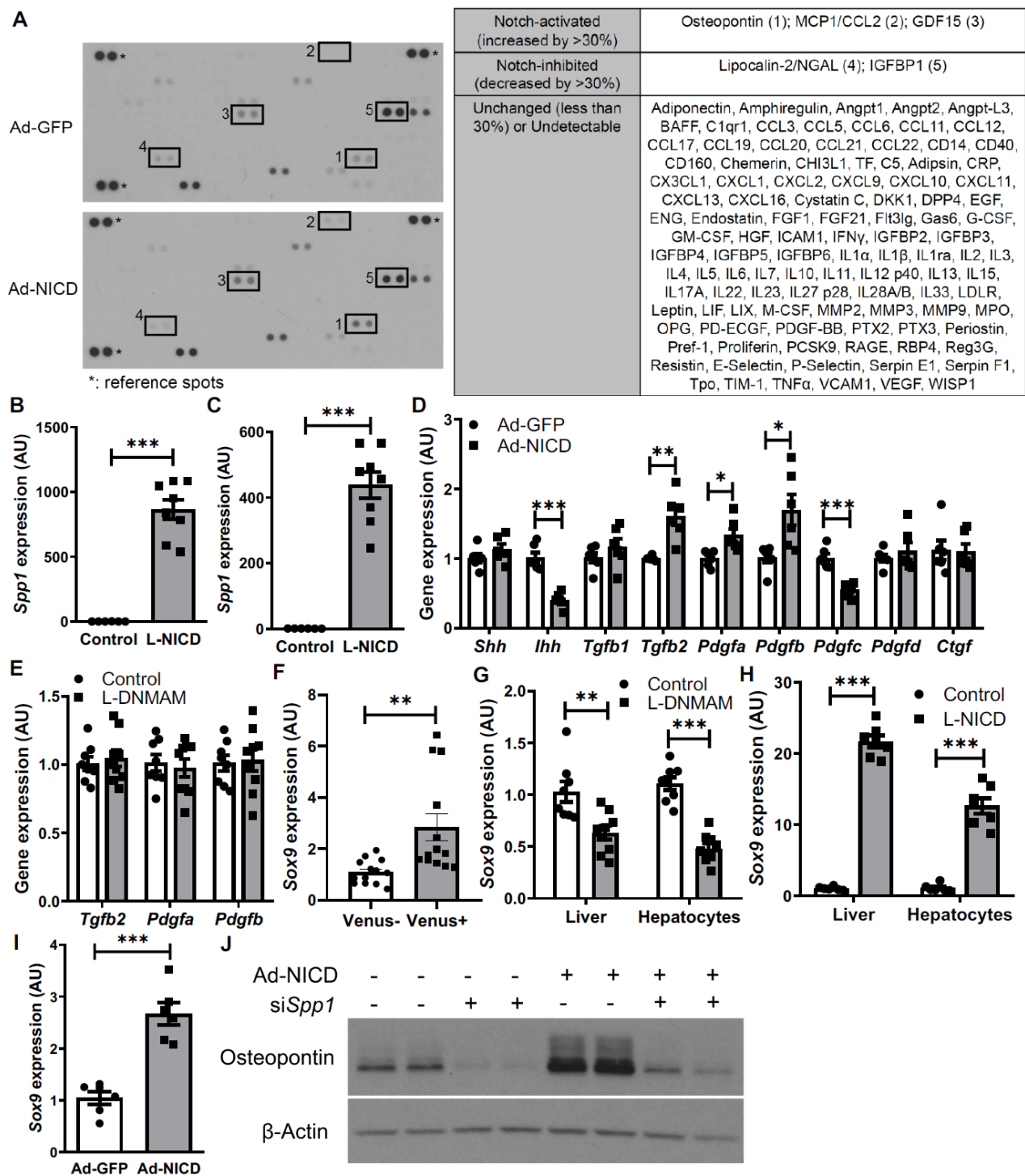
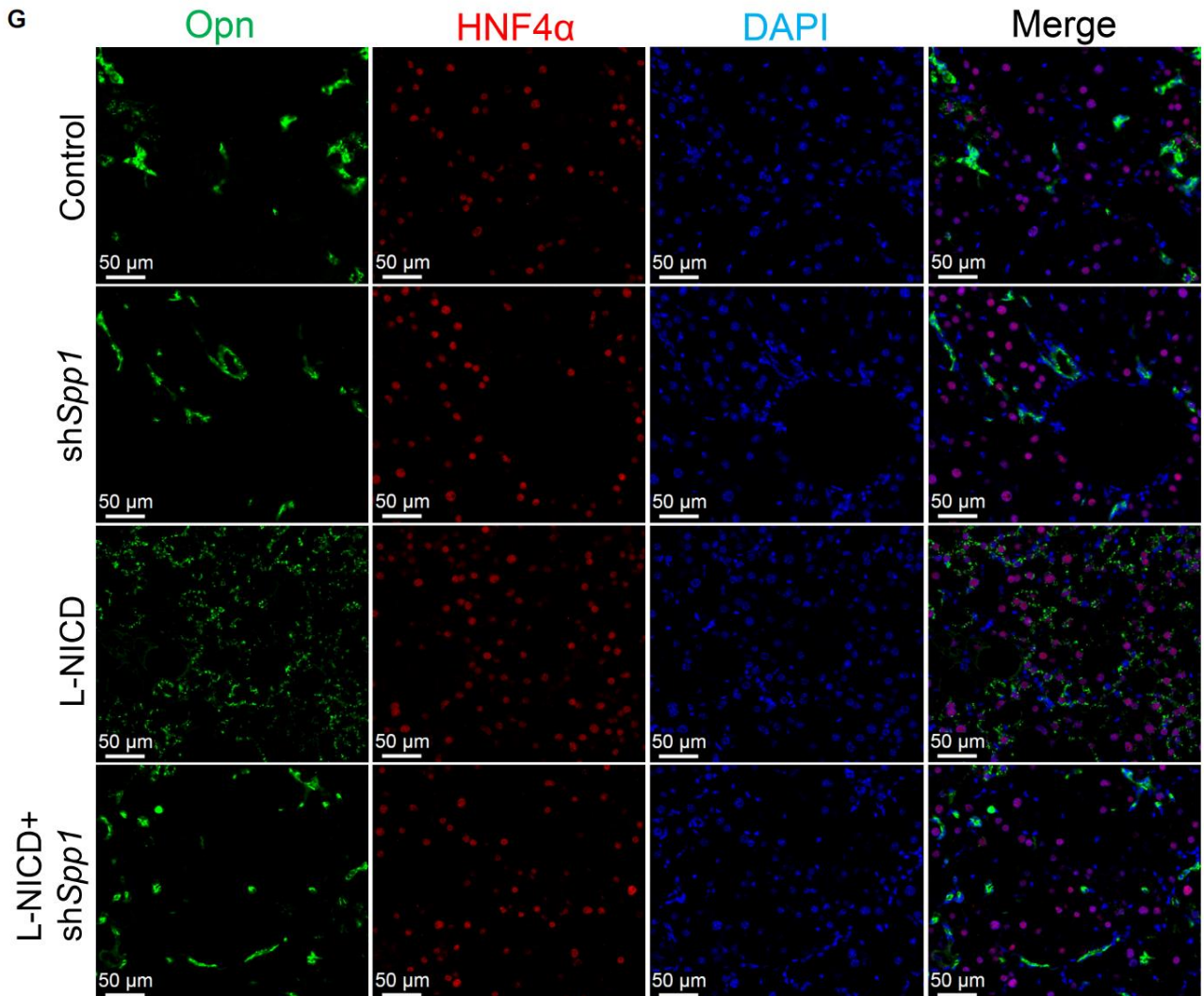
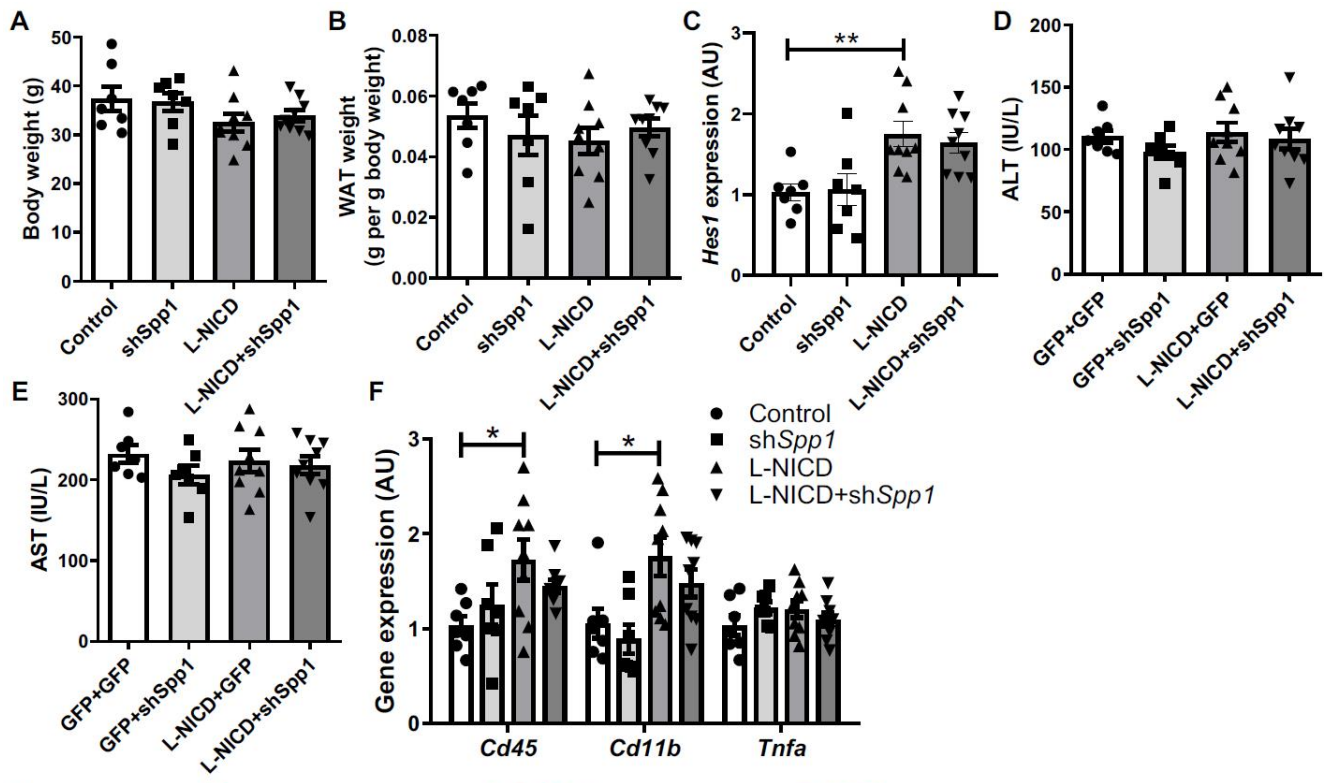


Fig. S11. Hepatocyte Notch activity regulates *Spp1* and *Sox9* expression. (A) Representative cytokine array of conditioned medium collected from control (Ad-GFP) and Ad-NICD-transduced primary hepatocytes (left) and all 111 cytokines examined in the array organized by Notch responsiveness (right). (B) Liver *Spp1* expression in chow-fed *L-NICD* male and (C) female mice ($n = 6$ to 8 per group). (D) Expression of other fibrogenic factors in Ad-NICD-transduced hepatocytes ($n = 6$

per group), with **(E)** confirmation of Notch-increased factors (from **fig. S11D**) in hepatocytes isolated from NASH diet-fed *L-DNMAM* mice ($n = 8$ per group). **(F to I)** *Sox9* expression in **(F)** Notch-inactive (*Venus*⁻) and Notch-active (*Venus*⁺) hepatocytes isolated from NASH diet-fed Notch reporter mice ($n = 13$ per group), **(G)** livers and isolated hepatocytes from NASH diet-fed *Cre*⁻ and *L-DNMAM* mice ($n = 8$ per group), **(H)** livers and isolated hepatocytes from *Cre*⁻ and *L-NICD* mice ($n = 7$ per group) and **(I)** Ad-NICD-transduced WT mouse primary hepatocytes ($n = 6$ per group). **(J)** Representative Western blots for Opn protein in primary hepatocytes transfected with control siRNA or si*Spp1*. * $P < 0.05$, ** $P < 0.01$, *** $P < 0.001$ as compared to the indicated controls by 2-tailed *t* tests (2 groups). NS, not significant. AU, arbitrary unit. Data are shown as the means \pm SEM.



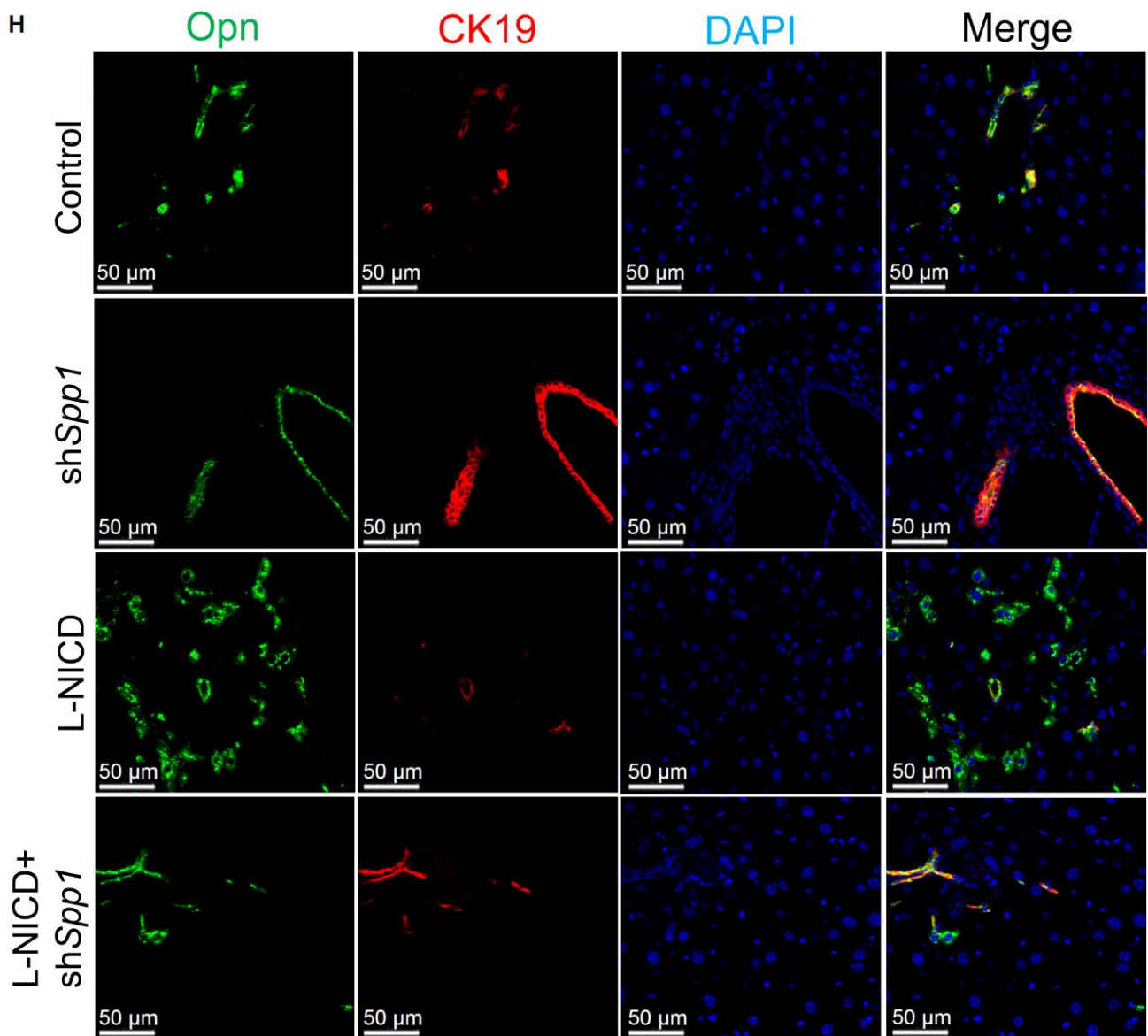


Fig. S12. Additional characterization of AAV8-H1-shSpp1-transduced mice. (A) Body weight, (B) epididymal WAT weight, (C) liver Notch activity, (D) serum ALT and (E) AST, (F) liver inflammatory gene expression and (G, H) representative staining images from NASH diet-fed Cre⁻ and L-NICD mice transduced with AAV8-H1-shControl or AAV8-H1-shSpp1 ($n = 7$ to 9 per group). * $P < 0.05$ and ** $P < 0.01$ as compared to the indicated controls by one-way ANOVA followed by post-hoc t tests (more than 2 groups). AU, arbitrary unit. Data are shown as the means \pm SEM.

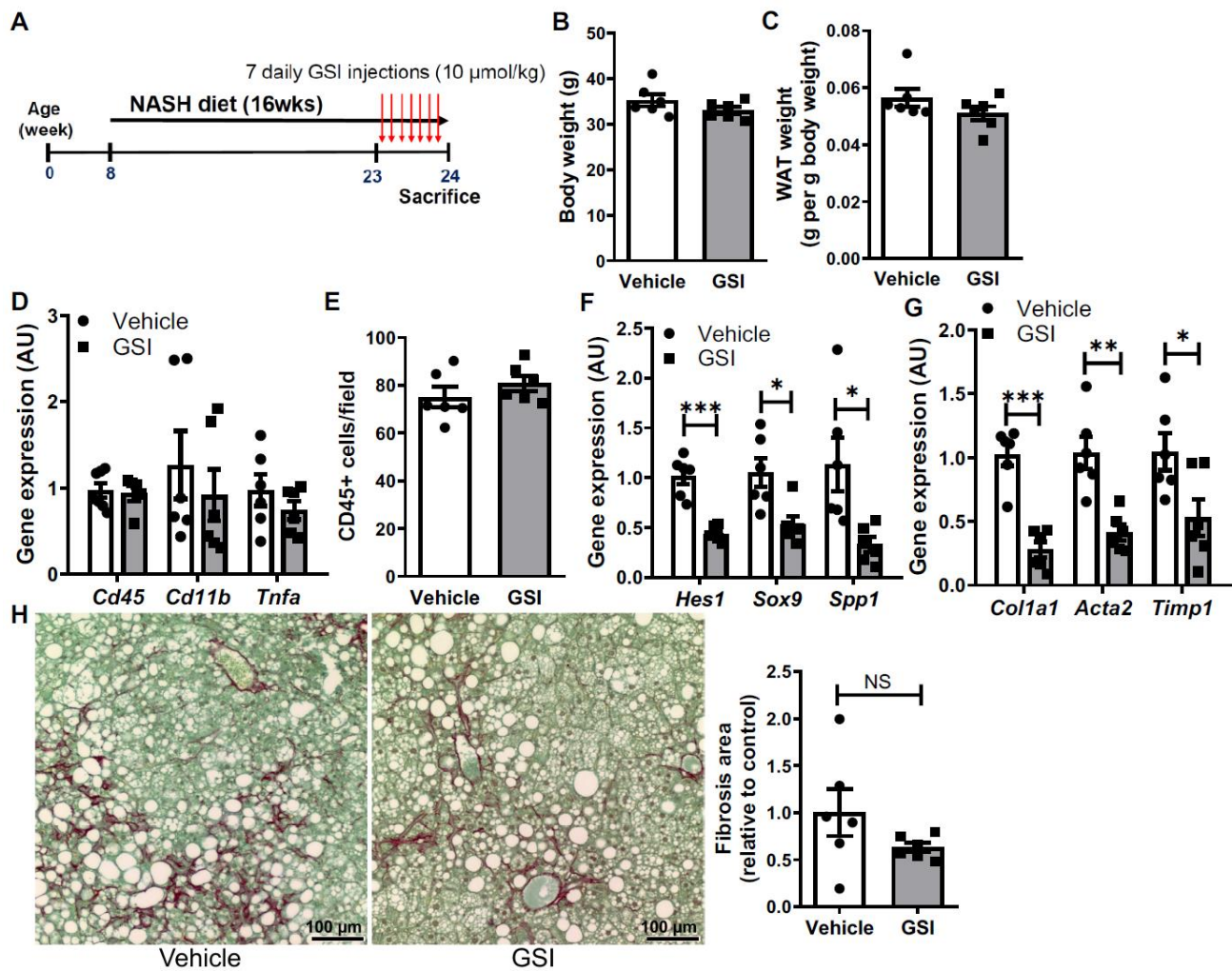


Fig. S13. Characterization of GSI-treated, NASH diet–fed mice. (A) WT mice were injected with vehicle or γ -secretase inhibitor (GSI) at 10 $\mu\text{mol/kg}$ once daily for 1 week after 15 weeks of NASH-feeding. (B) Body weight, (C) epididymal WAT weight, (D) liver inflammatory gene expression, (E) CD45⁺ cell infiltrate, (F) Notch target and (G) fibrogenic gene expression and (H) liver collagen content in vehicle- and acute GSI-treated mice ($n = 6$ per group). * $P < 0.05$, ** $P < 0.01$ and *** $P < 0.001$ as compared to vehicle-injected controls by 2-tailed t tests (2 groups). NS, not significant. AU, arbitrary unit. All data are shown as the means \pm SEM.

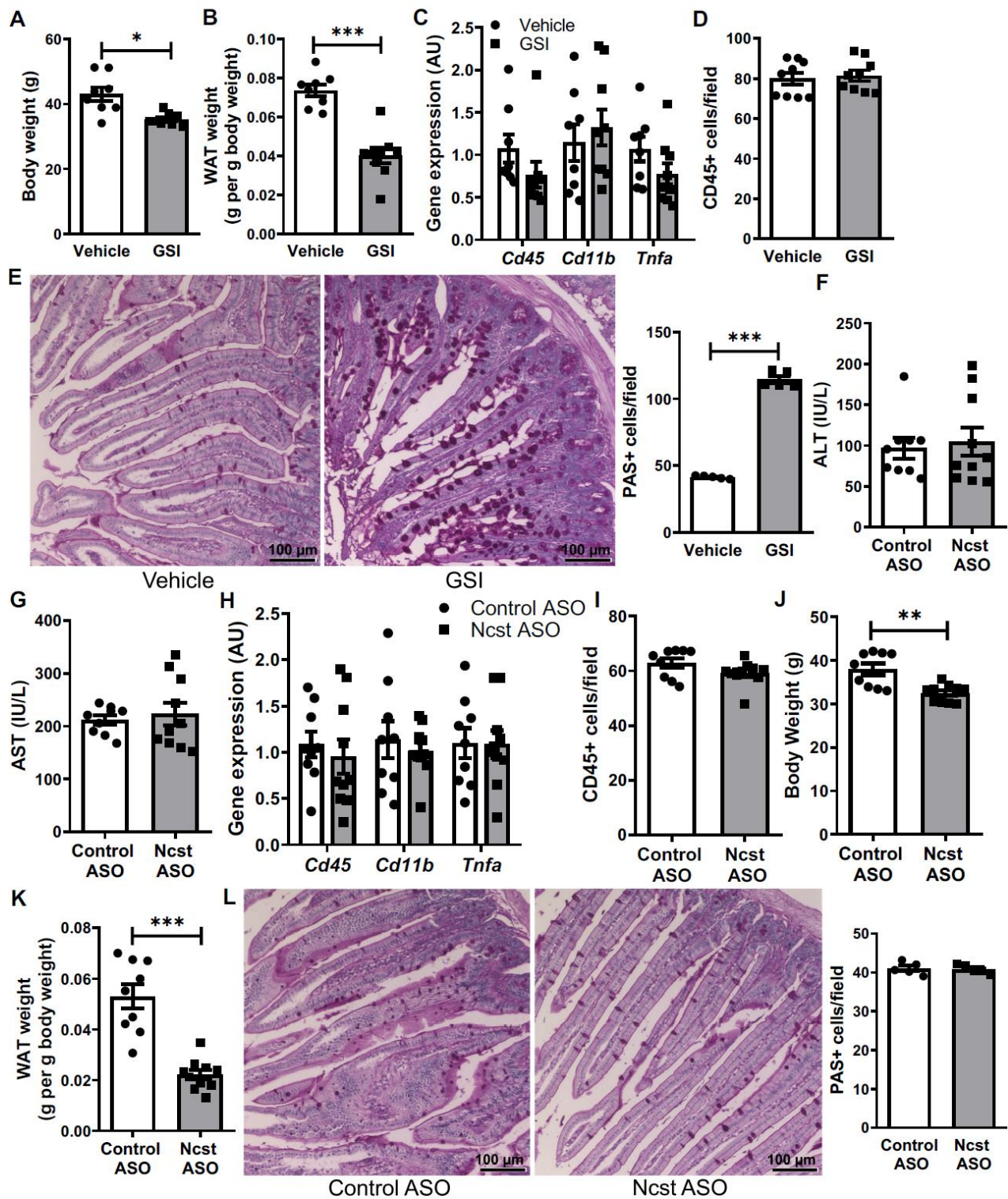


Fig. S14. Additional characterization of GSI- and ASO-treated mice. (A) Body weight, (B) epididymal WAT weight, (C) liver inflammatory gene expression and (D) CD45⁺ cell infiltrate in vehicle- and chronic GSI-treated NASH diet-fed WT mice ($n = 8$ to 9 per group). (E) Goblet cell metaplasia, indicated by increased small intestine PAS staining with GSI treatment ($n = 5$ per group). (F) Serum

ALT and **(G)** AST, **(H)** liver inflammatory gene expression and **(I)** CD45⁺ cell infiltrate, **(J)** body weight, **(K)** epididymal WAT weight in WT mice treated with either control or *Ncst* ASO ($n = 9$ to 10 per group). **(L)** small intestine PAS staining with quantitation of intestinal goblet cell number in control or *Ncst* ASO-treated mice ($n = 5$ per group). * $P < 0.05$ and *** $P < 0.001$ as compared to the indicated controls by 2-tailed t tests (2 groups). AU, arbitrary unit. All data are shown as the means \pm SEM.

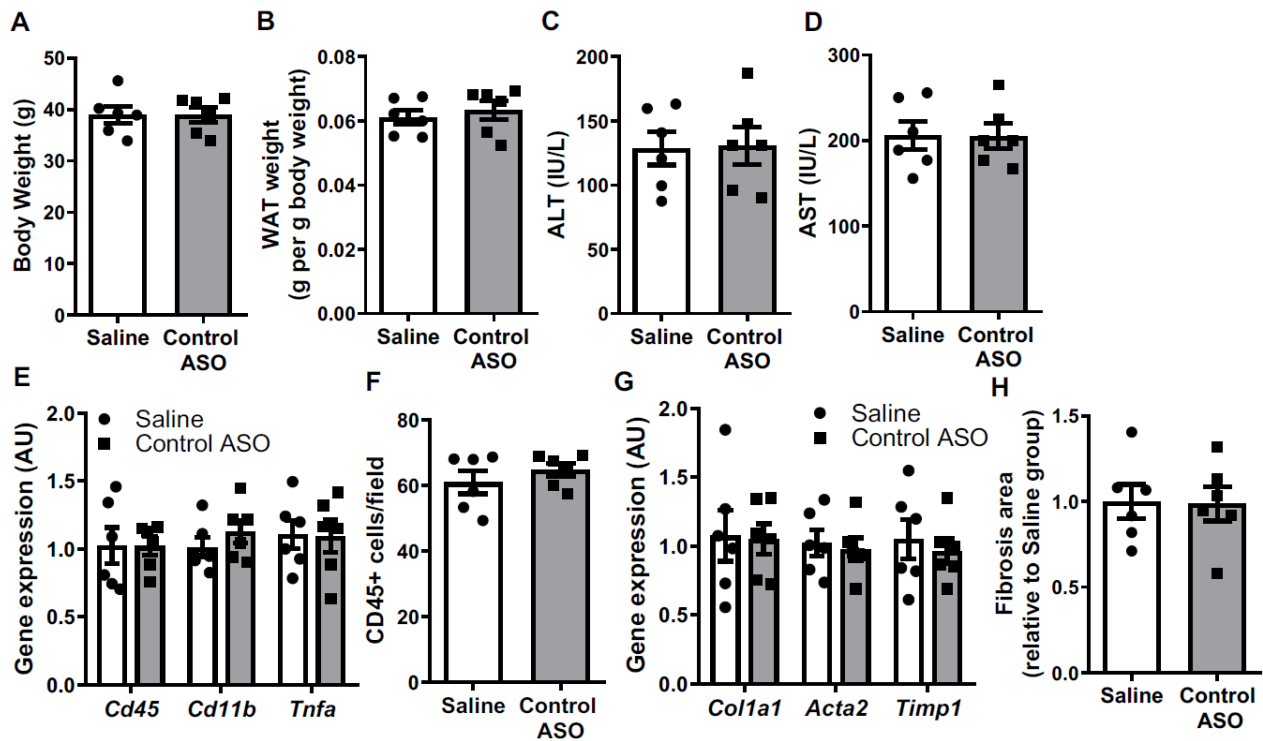


Fig. S15. Comparison of saline- and control ASO-treated mice. (A) Body weight, (B) epididymal WAT weight, (C) serum ALT and (D) AST, (E) liver inflammatory gene expression, (F) CD45⁺ cell infiltrate, (G) fibrogenic gene expression, and (H) liver collagen content in NASH diet-fed WT mice injected with saline and control ASO (25 mg/kg for 8 weeks), $n = 6$ per group. 2-tailed t tests were performed to compare the two groups. AU, arbitrary unit. All data are shown as the means \pm SEM.

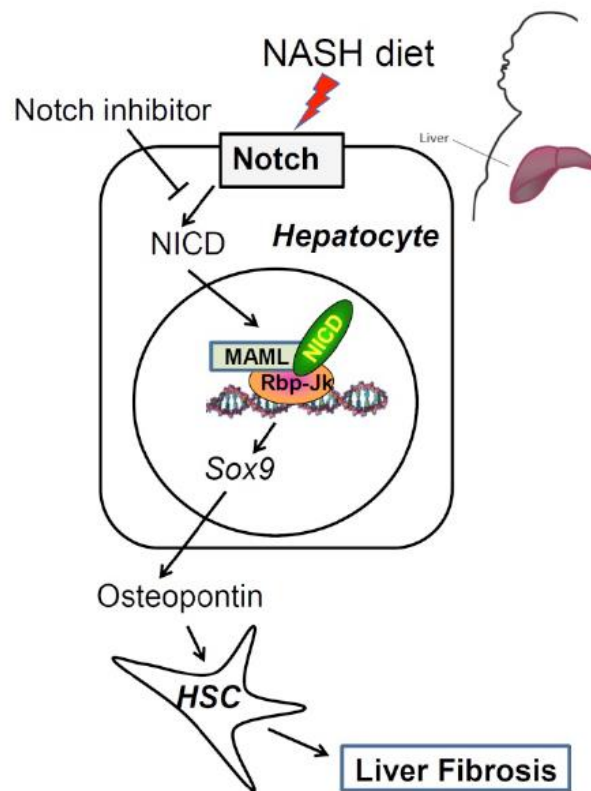


Fig. S16. Model of hepatocyte Notch action to increase NASH-associated fibrosis. Hepatocyte Notch is aberrantly activated in human and mouse NASH, which increases expression and secretion of Opn via the Notch-responsive transcription factor Sox9. Opn activates hepatic stellate cells (HSCs) and induces NASH-associated fibrosis that can be targeted by Notch inhibitors.

Table S1. Demographic and clinical features of PIVENS patients.

Cross-sectional study (n = 118, 72F/46M)			
	NR	R	<i>P</i> -value
Number	49	69	
Gender (female)	31	41	
Age (years)	46.9 ± 13.4	47.5 ± 12.0	0.786
BMI (kg/m ²)	36.3 ± 6.80	34.7 ± 7.42	0.238
NAS	4.84 ± 1.30	2.52 ± 1.09	9.03*10 ⁻¹⁷
Fibrosis Score	1.71 ± 1.06	0.91 ± 1.13	1.51*10 ⁻⁴
ALT (IU/L)	59.5 ± 28.1	36.1 ± 21.7	5.24*10 ⁻⁶
HOMA-IR	6.07 ± 5.56	3.90 ± 2.78	0.0163

Longitudinal study (n = 21, 10F/11M)						
	Pre-treatment			End-of-treatment		
	NR	R	<i>P</i> -value	NR	R	<i>P</i> -value
Number	10	11		10	11	
Gender (female)	5	5		5	5	
BMI (kg/m ²)	37.3 ± 8.33	37.5 ± 9.55	0.952	38.3 ± 7.53	37.5 ± 8.93	0.829
NAS	4.10 ± 1.45	4.64 ± 1.43	0.405	4.80 ± 1.40	2.82 ± 0.874	0.00160
Fibrosis Score	1.40 ± 1.07	1.00 ± 1.18	0.427	1.60 ± 0.843	0.55 ± 0.934	0.0136
ALT (IU/L)	82.8 ± 58.7	86.6 ± 56.7	0.881	67.4 ± 23.1	40.1 ± 21.1	0.0112
HOMA-IR	5.00 ± 2.37	5.54 ± 3.65	0.693	4.85 ± 3.02	4.44 ± 3.06	0.768

Values are means ± SD. F: female; M: male; NR: nonresponders; R: responders; BMI: body mass index; NAS: NALFD activity score; HOMA-IR: homeostatic model assessment of insulin resistance. *P*-values were generated by two-tailed Student's *t*-test between NR and R groups.

Table S2. Demographic and clinical features of patients with suspected NASH.

	Biopsy cohort (N = 159)
Age, years	45 ± 10
Sex, female	95 (60%)
BMI, Kg/m ²	37.8 ± 8.5
IFG/T2DM	41 (26%)
Glucose, mmol/l	5.6 ± 1.8
Total cholesterol, mmol/l	5.3 ± 1.0
LDL cholesterol, mmol/l	3.2 ± 1.0
HDL cholesterol, mmol/l	1.3 ± 0.4
Triglycerides, mmol/l	1.6 ± 1.0
ALT, IU/l	28 [18-57]
AST, IU/l	22 [17-33]

Values are means ± SD, median [interquartile range], or number (%). BMI: body mass index; IFG: impaired fasting glucose; T2DM: type 2 diabetes mellitus; LDL: low-density lipoprotein; HDL: high-density lipoprotein.

Table S3. Sequences of quantitative polymerase chain reaction primers used in the experiments.

Gene	Primers
<i>18S</i> forward (human)	5'-AAACGGCTACCACATCCAAG-3'
<i>18S</i> reverse (human)	5'-CCTCCAATGGATCCTCGTTA-3'
<i>ACTB</i> forward (human)	5'-AAGAGCTACGAGCTGCCTGA-3'
<i>ACTB</i> reverse (human)	5'-TCCATGCCAGGAAGGAAGG-3'
<i>HES1</i> forward (human)	5'-CAACACGACACCGGATAAACCA-3'
<i>HES1</i> reverse (human)	5'-TGCCGCGAGCTATCTTTCTTC-3'
<i>HEYL</i> forward (human)	5'-AGCCTGCGTTCGCCATGAA-3'
<i>HEYL</i> reverse (human)	5'-CTATGATCCCTCTGCGTTTCTTC-3'
<i>SPP1</i> forward (human)	5'-TTGCAGCCTTCTCAGCCAAA-3'
<i>SPP1</i> reverse (human)	5'-CAGCCTGTTAACTGGTATGGCAC-3'
<i>36b4</i> forward (mouse)	5'-GGAGAAACTGCTGCCTCACA-3'
<i>36b4</i> reverse (mouse)	5'-AGCAGCTGGCACCTTATTGG-3'
<i>Acta2</i> forward (mouse)	5'-CAGCCATCTTTCATTGGGATGGAG-3'
<i>Acta2</i> reverse (mouse)	5'-AATGCCTGGGTACATGGTGG-3'
<i>Cd11b</i> forward (mouse)	5'-CTCACGTATCCGTGCCTTCTT-3'
<i>Cd11b</i> reverse (mouse)	5'-GTCCACGCAGTCCGGTAAA-3'
<i>Cd45</i> forward (mouse)	5'-ACTGAGCACAAACAGAGAATGCC-3'
<i>Cd45</i> reverse (mouse)	5'-AGCGTGGATAACACACCTGGA-3'
<i>Col1a1</i> forward (mouse)	5'-GAACTGGACTGTCCCAACCC-3'
<i>Col1a1</i> reverse (mouse)	5'-TTGGGTCCCTCGACTCCTAC-3'
<i>Ctgf</i> forward (mouse)	5'-AGAAGTGTGTACGGAGCGTG-3'
<i>Ctgf</i> reverse (mouse)	5'-GGTGCACCATCTTTGGCAGT-3'
<i>Hes1</i> forward (mouse)	5'-ACGACACCGGACAAACCAA-3'
<i>Hes1</i> reverse (mouse)	5'-GAATGCCGGGAGCTATCTTTCT-3'
<i>Ihh</i> forward (mouse)	5'-ACCTCAGACCGTGACCGAAA-3'
<i>Ihh</i> reverse (mouse)	5'-GGCCGAATGCTCAGACTTGAC-3'
<i>Krt19</i> forward (mouse)	5'-AGTCCCAGCTCAGCATGAAAG-3'
<i>Krt19</i> reverse (mouse)	5'-CAGCTGGACTCCATAACGGG-3'
<i>Nicastrin</i> forward (mouse)	5'-AATGGAGAAGCTGAAGGGAAC-3'
<i>Nicastrin</i> reverse (mouse)	5'-CCCGTAGGAGTTGGAGTAAATAC-3'
<i>Notch1</i> forward (mouse)	5'-CAGACCAACACGCAGTACCA-3'
<i>Notch1</i> reverse (mouse)	5'-GACGTCAATGCCTCGCTTCT-3'
<i>Notch2</i> forward (mouse)	5'-GCTATGGCCAACAGTAACCCT-3'
<i>Notch2</i> reverse (mouse)	5'-GCGTAGCCCTTCAGACACTC-3'
<i>Notch3</i> forward (mouse)	5'-TGTGCTACAGCCGTGTGTTT-3'
<i>Notch3</i> reverse (mouse)	5'-CACAAGAGGCCTGTCTTCCC-3'
<i>Notch4</i> forward (mouse)	5'-ACCAGAGAGCTTCTGTGTGGAG-3'
<i>Notch4</i> reverse (mouse)	5'-CACTGGCAGATCCCTTGTCC-3'
<i>Pdgfa</i> forward (mouse)	5'-GAGGAGGAGACAGATGTGAGGT-3'
<i>Pdgfa</i> reverse (mouse)	5'-GAACAAAGACCGCACGCAC-3'
<i>Pdgfb</i> forward (mouse)	5'-TGCACAGAGACTCCGTAGATGA-3'

<i>Pdgfb</i> reverse (mouse)	5'-CACTCGGCGATTACAGCAGG-3'
<i>Pdgfc</i> forward (mouse)	5'-CCAGTCAGCCAAATGCTCCT-3'
<i>Pdgfc</i> reverse (mouse)	5'-GGATCTTGCACTCCGTTCTGT-3'
<i>Pdgfd</i> forward (mouse)	5'-AACCTCAGGAGAGATGAGAGCA-3'
<i>Pdgfd</i> reverse (mouse)	5'-AGCCACCATGTCAGAAGCAG-3'
<i>Shh</i> forward (mouse)	5'-CAACGTAGCCGAGAAGACCC-3'
<i>Shh</i> reverse (mouse)	5'-TGCACCTCTGAGTCATCAGCC-3'
<i>Sox9</i> forward (mouse)	5'-TCTGGAGGCTGCTGAACGAG-3'
<i>Sox9</i> reverse (mouse)	5'-GCTTGTCCGTTCTTCACCGA-3'
<i>Spp1</i> forward (mouse)	5'-CCTGGCTGAATTCTGAGGGAC-3'
<i>Spp1</i> reverse (mouse)	5'-CAGTCACTTTACCGGGAGG-3'
<i>Tbp</i> forward (mouse)	5'-CACAGGAGCCAAGAGTGAAGAA-3'
<i>Tbp</i> reverse (mouse)	5'-GCCTTCCAGCCTTATAGGGAAC-3'
<i>Tgfb1</i> forward (mouse)	5'-GCCCGAAGCGGACTACTATG-3'
<i>Tgfb1</i> reverse (mouse)	5'-ATAGATGGCGTTGTTGCGGT-3'
<i>Tgfb2</i> forward (mouse)	5'-ATAATTGCTGCCTTCGCCCTC-3'
<i>Tgfb2</i> reverse (mouse)	5'-AGGCTGAGGACTTTGGTGTGT-3'
<i>Timp1</i> forward (mouse)	5'-ACTCGGACCTGGTCATAAGGG-3'
<i>Timp1</i> reverse (mouse)	5'-CGCTGGTATAAGGTGGTCTCGT-3'
<i>Tnfa</i> forward (mouse)	5'-CCCACGTCGTAGCAAACCA-3'
<i>Tnfa</i> reverse (mouse)	5'-TCTTTGAGATCCATGCCGTTGG-3'